Environment and Ecology 43 (2) : 375—384, April—June 2025
Article DOI: https://doi.org/10.60151/envec/TRPP7406
ISSN 0970-0420

Antioxidant and Antimicrobial Activities of Silver and Iron Nanoparticles Synthesized from Jackfruit Peel (*Artocarpus heterophyllus*): A Sustainable Waste Valorization Approach

Anjana K., Abhirami M., Sarah Jane Monica, Sivaraj C.

Received 30 January 2025, Accepted 19 March 2025, Published on 16 April 2025

ABSTRACT

Effective management of fruit peel waste is essential for environmental sustainability. Utilizing these waste substrates for nanoparticle (NP) synthesis presents a sustainable approach. The green synthesis of NPs using fruit peels has garnered attention due to its cost efficiency and eco-friendly nature. This study investigates the antioxidant and antimicrobial properties of silver and iron nanoparticles synthesized from jackfruit peel extract (*Artocarpus heterophyllu*s). NPs were characterized using UV-vis spectroscopy, FTIR, and SEM analysis. Antioxidant activity was assessed through DPPH, $ABTS^{\bullet+}$, Superoxide, FRAP, and phosphomolybdenum assays. Antibacterial activity was tested against gram-positive (*Enterococcus faecalis, Streptococcus mutans*, and *Staphylococcus aureus*) and gram-negative (*Bacillus subtilis, E. coli, Pseudomonas aeruginosa*) bacterial strains. Antifungal activity was evaluated against *Candida krusei, C. tropicalis,* and *C. albicans.* A distinct color change from yellow to brown, coupled with a peak in the UV spectrum at 425 nm, confirmed the formation of AgNPs. Similarly, the formation of FeNPs was confirmed by a color change from yellow to black and a peak in the UV spectrum at 213 nm. The average particle size of AgNPs ranged from 45.0 to 72.1 nm, while FeNPs measured between 4.9 and 30.9 nm. FeNPs exhibited significantly better antioxidant activity, with IC_{50} values of 109.23, 54.98, and 61.56 µg/mL for DPPH, ABTS, and superoxide radical assays ($p<0.05$). In contrast, AgNPs demonstrated better antibacterial activity with a maximum zone of inhibition recorded for *S. mutans* (24 mm) and *C. tropicalis* (16 mm) while antifungal activity was observed only for AgNPs. Results indicate that NPs synthesized from jackfruit peel extract have antioxidant and antimicrobial activities, making this fruit peel a suitable medium for eco-friendly nanoparticle production.

Keywords Nanoparticles, Fruit peels, *Artocarpus heterophyllus,* Antioxidant, Antimicrobial.

Anjana K.[1], Abhirami M.[2], Dr Sarah Jane Monica[3]*, Sivaraj C.[4],

[3]Assistant Professor
[1,2,3]Department of Food Science, M. O. P. Vaishnav College for Women (Autonomous), Chennai 600034, Tamil Nadu, India

[4]Scientist
Department of Phytochemistry Vopec Pharmaceuticals, Chennai, Tamil Nadu, India

Email: : sarahjanemonica.fsm@mopvaishnav.ac.in
*Corresponding author

INTRODUCTION

Fruits and vegetables are among the most widely consumed horticultural products. The processing

of fruits and vegetables generates waste in the form of pomace, peels, rinds, and seeds, which account for 25–30% of total produce. These by-products generated from industries, and household kitchens, are rich in valuable bioactive compounds, dietary fiber, essential micronutrients, and oils (Kumar *et al.* 2020). However, they are often discarded improperly, leading to environmental issues. Fruit peels serve as a valuable source of bioactive compounds, from which natural antioxidants and antimicrobial agents can be extracted (Nirmal *et al.* 2023). Recently, there has been a growing focus on valorizing these low-cost horticultural wastes for diverse applications. Nanotechnology is experiencing significant growth in interdisciplinary research and provides innovative solutions for waste valorization. Fruit peels are emerging as novel precursor agents for synthesizing various nanoparticles (NPs) while also contributing to the reduction of agricultural by-products (Suhag *et al.* 2022, Rodriguez-Felix *et al.* 2023). Research indicates that different metal oxide NPs can be derived from waste materials produced by fruits such as pomegranates, oranges, and apples (Leta *et al.* 2024).

Artocarpus heterophyllus (jackfruit), a member of the Moraceae family, is a tropical climacteric fruit known for its versatility and distinctive sweet flavor. It is extensively cultivated across Asia, Africa, and South America (Ranasinghe *et al.* 2019). The underutilized parts of this fruit include the peel, perianth, rind, and outer core. The jackfruit peel (JFP), which constitutes approximately 60% to 70% of the fruit's mass, features as a spiked exterior and is typically regarded as a waste byproduct (Adan *et al*. 2020). JFP is sometimes used as a cattle feed containing carbohydrates, proteins, and fat. JFP is a rich source of bioactive compounds, including steroids, triterpenoids, saponins, alkaloids, glycosides, tannins, polyphenols, and flavonoids (Brahma and Ray 2022). Furthermore, peel extracts are abundant in pectin (8.94% to 15.14%), making them valuable as emulsifiers, binders, and stabilizers in the food and pharmaceutical industries (Xu *et al.* 2018).

Recently, considerable interest has been in utilizing solid residues, particularly peels and seeds produced by the fruit and vegetable industries, in synthesizing NPs. Although rich in phytochemicals, JFP is frequently discarded disorderly, contributing to significant environmental challenges. However, strategically using these by-products can enhance their economic value and simultaneously reduce disposal costs. Thus, the study aimed to evaluate the antioxidant and antimicrobial activities of silver and iron NPs synthesized using JFP.

MATERIALS AND METHODS

Plant materials and chemicals

Jackfruits were sourced from the Koyambedu fruit market, Chennai during the peak maturation season (April – May 2024). All the chemicals utilized were of analytical grade and procured from Sigma Aldrich. Distilled water was used consistently throughout the study.

Preparation of peel extract

Jackfruits were thoroughly washed with tap and distilled water to remove dirt particles and impurities. The peels were carefully removed, rinsed thrice using distilled water, and cut into small pieces. To prepare the aqueous extract, 25 g of jackfruit peel was mixed with 150 mL of distilled water in a 250 mL conical flask. This mixture was heated at 70ºC for 30 min. After cooling, the solution was filtered through Whatman No. 1 filter paper. The resulting filtered extract was stored in glass bottles for subsequent synthesis of NPs.

Synthesis of NPs

AgNPs: To synthesize AgNPs, aqueous peel extract was combined with 0.1M $AgNO_3$ (3:2 ratio) to reduce silver ions. The mixture was exposed to sunlight for 10 min and incubated in the dark for 24 h. The solution was centrifuged at 6,000 rpm for 10 minutes, the supernatant was discarded, and the remaining pellets were transferred to a petri dish and dried at room temperature for 48 h.

FeNPs: To synthesize FeNPs, aqueous peel extract was combined with 0.1M $FeCl_2$ (3:2 ratio), and the pH was adjusted to 6.0 by adding NaOH. This solution

was continuously stirred at 60ºC until a black solid precipitate was obtained. The precipitate was centrifuged at 6000 rpm for 15 min, washed with ethanol, and dried in a hot air oven at 60ºC.

Characterization of NPs

UV–Vis Spectroscopy: Visual changes in the reaction mixtures were first observed, followed by spectrophotometric analysis to confirm the synthesis of NPs. The optical properties of the synthesized NPs were evaluated using a UV–Vis spectrophotometer (SPECTRO x SORT 2000, High Resolution, India). Scans were performed within the wavelength range of 200–800 nm at a resolution of 1 nm. Double-distilled water was used as the blank reference.

Fourier transform infra-red spectroscopy (FTIR): FTIR was employed to identify the bio-functional groups from JFP responsible for reducing NPs. The FTIR spectra were recorded over the range of 500–3400 cm^{-1} with a resolution of 1 cm^{-1}. (BRUKER ALPHA II, India).

Scanning electron microscopy (SEM): SEM was used to study the size of the NPs.

Antioxidant activity: For all antioxidant assays, ascorbic acid served as the standard, and the optical density (OD) was measured spectrophotometrically using a UV-Vis 2000 spectrophotometer (Lab India).

DPPH (2, 2–diphenyl–1–picrylhydrazyl) radical scavenging assay: Various concentrations of AgNPs and FeNPs (20 to 120 µL) were combined with 1mL of freshly prepared 0.1mM DPPH methanolic solution. After 30 min of incubation in the dark at room temperature, the OD was measured at 517 nm (Begam *et al.* 2020). Results are expressed as % inhibition of DPPH free radical.

$$\% \text{ inhibition of DPPH free radical} = [(A_C\text{-}A_S/A_C) \times 100]$$

A_C Corresponds to control absorbance
A_S Corresponds to sample absorbance

ABTS$^{\bullet+}$(2,2 2'-azino-bis-3-ethyl benzothiazole-6-sulphonic acid) radical scavenging assay: Varying concentrations of AgNPs and FeNPs (20 to 120 µL) were combined with 1 mL of freshly prepared ABTS$^{\bullet+}$ solution, and incubated for 5 - 10 min. The OD was measured at 734 nm (Sangeetha *et al.* 2020). Results are expressed as % inhibition of ABTS$^{\bullet+}$ radical

$$\% \text{ inhibition of ABTS}^{\bullet+} \text{ free radical} = [(A_C\text{-}A_S/A_C) \times 100]$$

A_C Corresponds to control absorbance
A_S Corresponds to sample absorbance

Superoxide (O_2-) radical scavenging assay: Varying concentrations of AgNPs and FeNPs (20 to 120 µL) were mixed with 1mL of reaction mixture containing phosphate buffer (50 mM, pH 7.4), 0.3 mL PMS (20 mM), NADH (150 mM), and NBT (50 mM). This solution was incubated for 15 min, after which OD was measured at 590 nm (Banu *et al*. 2021). Results are expressed as % inhibition of superoxide anion (O_2-) radical.

$$\% \text{ inhibition of } O_2- \text{ free radical} = [(A_C\text{-}A_S/A_C) \times 100]$$

A_C Corresponds to control absorbance
A_S Corresponds to sample absorbance

FRAP assay: Varying concentrations of AgNPs and FeNPs (20 to 120 µL) were mixed with 1 mL of PBS (0.2M; pH 6.6) and 1 mL 1% K_3 [Fe $(CN)_6$] (w/v). The solution was incubated in a thermostatic bath for 25 min at 50°C. After cooling, 1 mL 10% TCA (w/v) and 0.5 mL 0.1% freshly prepared $FeCl_3$ (w/v) were added. The OD was measured at 700 nm (Mzoughi *et al.* 2019). Results are expressed as % reduction of Fe^{3+} to Fe^{2+} ions.

Phosphomolybdenum reducing assay: Varying concentrations of AgNPs and FeNPs were (20 to 120 µL) mixed with 1mL of freshly prepared reagent solution [H_2SO_4 (0.6 M), Na_3PO_4 (28 mM), and $(NH_4)_2M_oO_4$ (4 mM)] and incubated for 90 min in a thermostatic bath at 95°C. After cooling, the OD was measured at 695 nm (Prieto *et al.* 1999). Results are expressed as a % reduction of Mo (VI) to Mo (V).

Antibacterial activity: Mueller Hinton Agar (MHA) was poured into sterile petri plates. A sterile disposable cotton swab was used to evenly spread the bacterial culture over the surface of the agar, which was then allowed to dry for 5 min. Five wells measuring 5 mm were created in the petri plates using a cork borer.

Three wells were filled with varying concentrations of AgNPs/FeNPs, one well with $AgNO_3/FeCl_2$, and the last well with a standard antibiotic (Tetracycline). After 30 min, the petri plates were incubated at 37°C for 24 hrs. The zone of inhibition was measured to the nearest mm using an antibiotic zone scale (Gabriel *et al.* 2022).

Antifungal activity: Potato Dextrose Agar (PDA) was poured into sterile petri plates. The fungal cultures were inoculated evenly on the surface of the solidified PDA plate. Five wells (each 5 mm in diameter) were created. Three wells were filled with varying concentrations of AgNPs/FeNPs, one well with $AgNO_3/FeCl_2$, and the last well with a standard antibiotic (Fluconazole). After 30 min, the petri plates were sealed with paraffin tape and incubated at 28°C for 48 hrs. The zone of inhibition was measured to the nearest mm using an antibiotic zone scale (Gizaw *et al*. 2022).

Statistical analyses: Data were analyzed using the Statistical Package for the Social Sciences (SPSS, version 24.0, IBM Corp., Endicott, NY, USA). Experiments were conducted in triplicate, and results are presented as mean ± standard deviation. Further analysis was performed using One-way analysis of variance (ANOVA) followed by Duncan's Multiple Range test.

RESULTS AND DISCUSSION

Nanotechnology is a promising multidisciplinary field dedicated to advancing organic and inorganic materials through manipulation at the atomic and molecular scale. NPs are generally categorized as carbon-based, inorganic, and organic-based NPs. Commonly synthesized inorganic metal NPs include silver (Ag), gold (Au), copper (Cu), iron (Fe), zinc (Zn), and cobalt (Co) (Khan *et al*. 2019). AgNPs and FeNPs have gained considerable attention due to their remarkable chemical, physical, and biological properties. These characteristics facilitate their extensive application across various scientific disciplines, particularly because of their antioxidant and antimicrobial properties (Fahmy *et al.* 2018, Magdy *et al*. 2024). Biologically produced NPs are gaining interest over physical and chemical methods

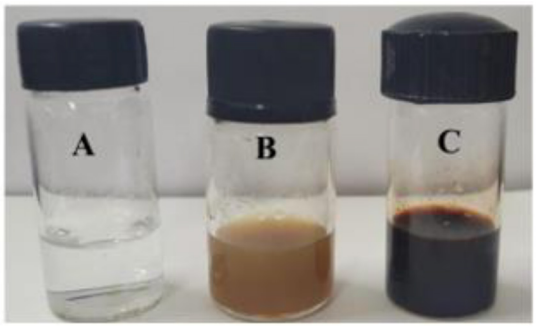

Fig. 1. A) $AgNO_3$ solution, B) JFP aqueous extract before adding $AgNO_3$, C) JFP aqueous tract after adding $AgNO_3$.

because they are safer, easier to synthesize, and have functional properties at lower concentrations. In this work, aqueous jackfruit peel extract (JFPE) was used to synthesize AgNPs and FeNPs, as JFPE is a rich source of phytochemicals that function as reducing agents for the synthesis of NPs. The formation of AgNPs and FeNPs from JFPE was monitored both visually and spectroscopically. A sharp color change from yellow to dark brown indicated the presence of AgNPs while a color change from yellow to black confirmed the presence of FeNPs (Figs. 1–2).

These eco-friendly synthesized NPs were further confirmed by recording their UV absorption spectrum in the 200–800 nm range. The appearance of distinct broad surface resonance peaks at 425 nm and 213 nm in the UV – vis spectra confirmed the presence of AgNPs and FeNPs (Figs. 3 –4).

The vibrational spectrum of a chemical molecule is a unique physical property that offers insights

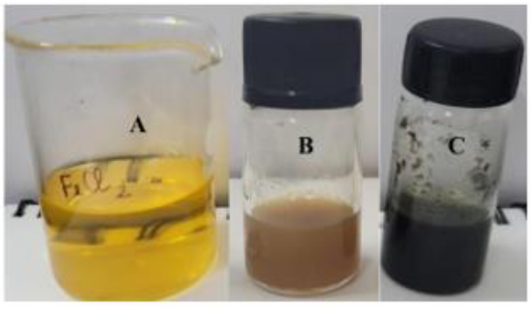

Fig. 2. A) $FeCl_2$ solution, B) JFP aqueous extract before adding $FeCl_2$, C) JFP aqueous extract after adding $FeCl_2$.

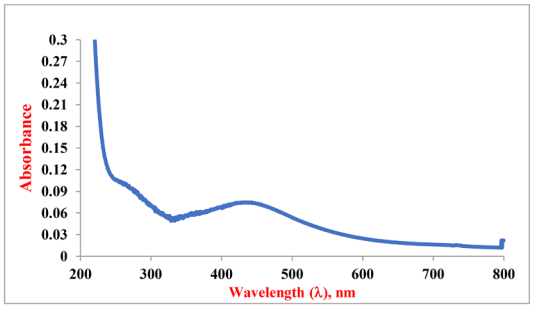

Fig. 3. UV visible spectrum of AgNPs.

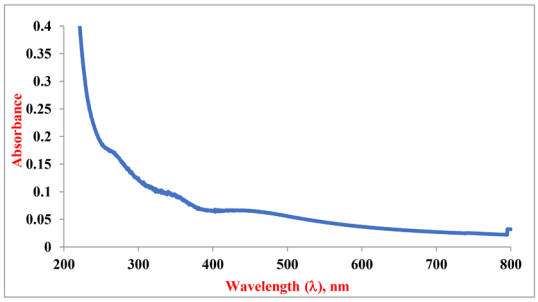

Fig. 4. UV visible spectrum of FeNPs.

into its structural and functional characteristics. The FTIR spectra of AgNPs and FeNPs were analyzed to ascertain their chemical composition and functional groups (Faghihi *et al.* 2020). Figure 5 presents the FTIR analysis of AgNPs synthesized using JFPE. A prominent peak at 3362 cm^{-1} corresponds to O–H stretching vibrations, indicating the presence of hydroxyl groups. The band at 2934 cm^{-1} is attributed to methylene C–H stretching, while the peak at 2108 cm^{-1} is associated with C=C stretching. Additional bands at 1985 cm^{-1}, 1913 cm^{-1}, and 1726 cm^{-1} are assigned to C=N, N=N, and C=O stretching vibrations, respectively. The peak at 1629 cm^{-1} is linked to alkenyl C=C stretching, reflecting unsaturated carbon bonding. Furthermore, the signals at 1315 cm^{-1} and 1071 cm^{-1} correspond to C–N stretching and CO–O–CO stretching (anhydride).

Figure 6 shows the FTIR analysis of FeNPs synthesized using JFPE. A prominent peak at 3307 cm^{-1} corresponds to O–H stretching vibrations, indicating the presence of hydroxyl groups. The band at 2940 cm^{-1} is attributed to methylene C–H stretching, while the peak at 2112 cm^{-1} is associated with C≡C stretching. Additionally, the peak at 1624 cm^{-1} reflects alkenyl C=C stretching, suggesting the presence of unsaturated carbon groups. The bands observed at 1258 cm^{-1}, 1050 cm^{-1}, and 1029 cm^{-1} are attributed to aromatic C–H stretching, CO–O–CO stretching (anhydride), and Fe–O bending vibrations (metal oxide), respectively. A peak at 587 cm^{-1} is linked to Fe stretching, while the signals at 558 cm^{-1} and 506 cm^{-1} correspond to alkyl halides and benzene derivatives. These findings highlight the essential role of phytochemical functional groups in the synthesis of AgNPs and FeNPs, aiding in their formation and stability.

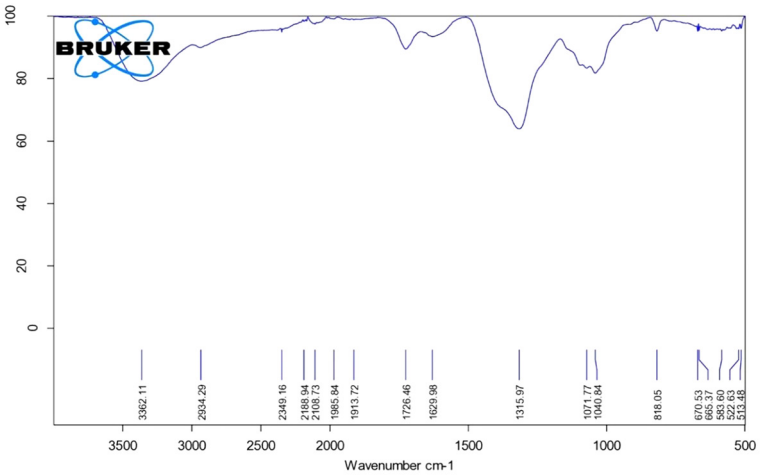

Fig. 5. FTIR spectral analysis of AgNPs.

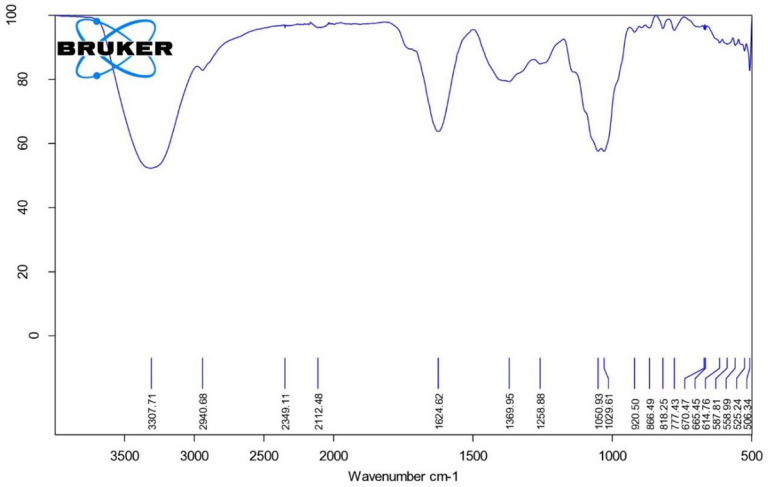

Fig. 6. FTIR spectral analysis of AgNPs.

The size and shape of the synthesized NPs were determined using SEM analysis. The average size of AgNPs ranged from 45.0 to 72.1 nm and FeNPs measured between 4.9 and 30.9 nm, with both types exhibiting spherical morphology (Figs. 7 –8).

Antioxidants protect cells from reactive oxygen species (ROS), which can cause oxidative damage. The *in vitro* results for free radical inhibition by the biosynthesized AgNPs and FeNPs are summarized and presented in Table 1. Both NPs effectively inhibited the action of free radicals in a concentration-dependent manner ($p<0.05$). The lower the IC_{50} value, the better the scavenging activity of antioxidant

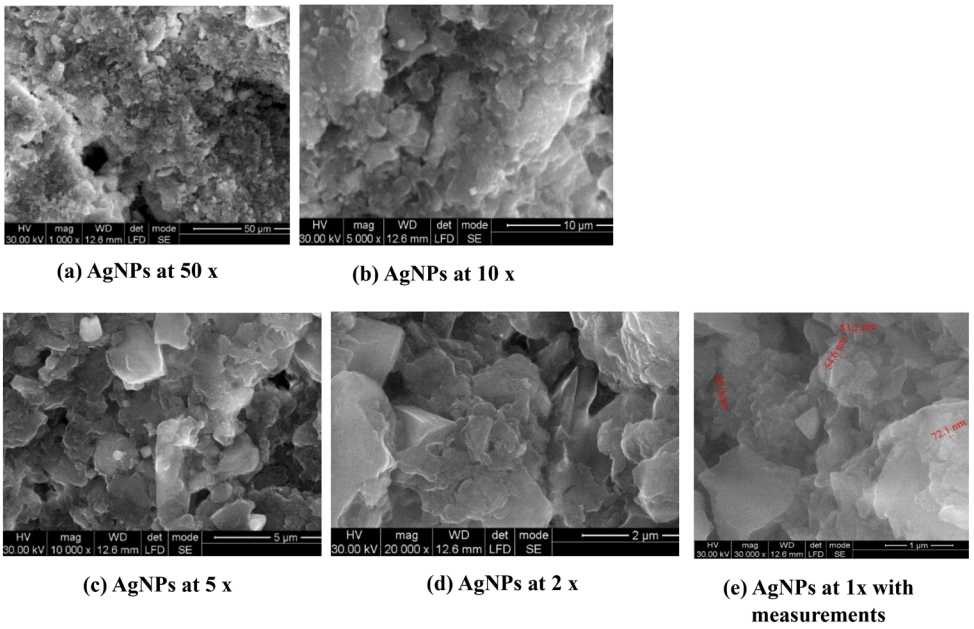

Fig. 7. SEM micrographs of AgNPs synthesized from JFP at different magnifications.

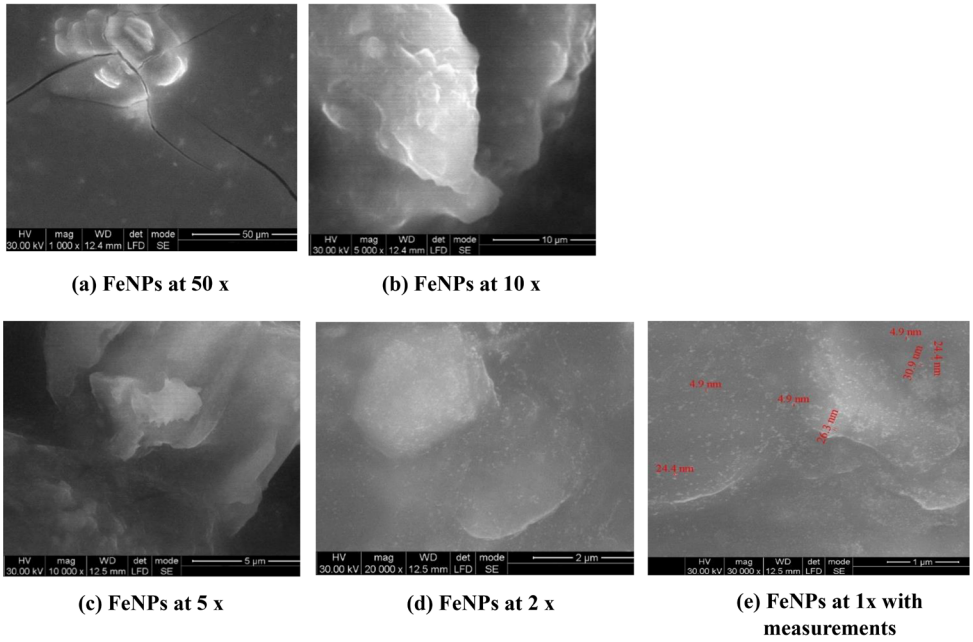

Fig. 8. SEM micrographs of FeNPs synthesized from JFP at different magnifications.

samples. Based on IC_{50} values, FeNPs showed the highest antioxidant properties, followed by AgNPs, and both were comparable to the positive control of ascorbic acid. The radical scavenging activity of the

Table 1. Radical scavenging activities of NPs synthesized from JFPE.

Concentration µg/mL	DPPH assay AgNPs	DPPH assay FeNPs	DPPH assay Ascorbic acid	$ABTS^{\bullet+}$ assay AgNPs	$ABTS^{\bullet+}$ assay FeNPs
20	4.22 ± 1.25 [a]	9.27 ± 5.66 [a]	62.04 ± 1.87 [b]	40.99 ± 2.22 [b]	8.68 ±1.35 [a]
40	7.21 ± 0.63 [a]	28.82 ± 3.13 [b]	67.62 ± 1.25 [c]	64.04 ± 1.51 [b]	12.27 ± 2.45 [a]
60	7.89 ± 0.85 [a]	32.45 ± 2.44 [b]	71.70 ± 2.66 [c]	71.37 ± 7.70 [b]	15.5 ± 2.25 [a]
80	11.56 ± 3.47 [a]	35.46 ± 1.15 [b]	78.77 ± 1.47 [c]	93.95 ± 0.80 [b]	72.75 ± 0.30 [a]
100	16.46 ± 4.77 [a]	39.85 ± 3.38 [b]	85.44 ± 2.25 [c]	96.57 ± 0.92 [b]	75.05 ± 0.92 [a]
120	20.01 ± 3.27 [a]	48.37 ± 2.26 [b]	89.39 ± 2.04 [c]	97.64 ± 1.51 [b]	83.53 ± 1.50 [a]
IC_{50} value	**305.49**	**109.23**	**16.13**	**24.43**	**54.98**

Table 1. Continued.

Concentration µg/mL	$ABTS^{\bullet+}$ assay Ascorbic acid	Superoxide assay AgNPs	Superoxide assay FeNPs	Superoxide assay Ascorbic acid
20	72.22 ± 1.85 [c]	32.35 ± 5.89 [a]	27.53 ± 6.64 [a]	55.22 ± 0.17 [b]
40	76.54 ± 2.33 [c]	40.20 ± 1.75 [a]	43.47 ± 11.5 [a]	61.46 ± 2.61 [b]
60	80.25 ± 2.33 [b]	44.12 ± 2.94 [a]	52.17 ± 13.04 [a]	74.46 ±1.52 [b]
80	83.95 ± 2.33 [c]	49.02 ± 1.70 [a]	59.42 ± 18.17 [a]	82.92 ±1.52 [b]
100	87.65 ± 1.41 [c]	53.92 ± 1.73 [a]	66.67 ± 17.57 [a]	87.72 ± 2.01 [b]
120	92.85 ± 2.78 [c]	58.82 ± 2.94 [a]	75.36 ± 15.27 [ab]	92.25 ± 1.25 [b]
IC_{50} value	**13.85**	**68.20**	**61.56**	**18.11**

Values are presented as mean ± SD (N=3). Mean values within a row for each assay that does not share a common letter are significantly different based on ANOVA and Duncan's Multiple Range Test ($P<0.05$).

Table 2. Reducing power of NPs synthesized from JFPE.

Concentration µg/mL	FRAP assay AgNPs	FeNPs	Ascorbic acid	Phosphomolybdenum assay AgNPs	FeNPs	Ascorbic acid
20	32.17 ± 0.20 [a]	33.60 ± 5.42 [a]	76.34 ± 1.08 [b]	86.41 ± 0.34 [c]	10.18 ± 2.50 [a]	82.97 ± 0.29 [b]
40	37.62 ± 0.16 [a]	37.38 ± 3.89 [a]	80.86 ± 1.26 [b]	91.76 ± 0.57 [c]	12.56 ± 2.86 [a]	84.20 ± 3.56 [b]
60	51.17 ± 0.40 [b]	42.47 ± 5.20 [a]	82.27 ± 0.19 [c]	92.85 ± 0.28 [c]	27.37 ± 2.23 [a]	84.80 ± 0.28 [b]
80	52.93 ± 0.07 [b]	44.30 ± 4.61 [a]	83.14 ± 0.26 [c]	93.10 ± 0.49 [c]	47.83 ± 0.46 [a]	85.98 ± 0.95 [b]
100	56.33 ± 0.06 [b]	72.68 ± 1.06 [a]	85.75 ± 0.35 [c]	93.17 ± 0.66 [c]	69.17 ± 0.30 [a]	86.93 ± 0.13 [b]
120	61.20 ± 0.04 [b]	78.39 ± 6.00 [a]	86.40 ± 0.15 [c]	94.01 ± 0.01 [c]	72.53 ± 1.16 [a]	88.32 ± 0.16 [b]

Values are presented as mean ± SD (N=3). Mean values within a row for each assay that does not share a common letter are significantly different based on ANOVA and Duncan's Multiple Range Test ($p<0.05$).

AgNPs and FeNPs was found to be in the following order: ABTS$^{\bullet+}$>Superoxide>DPPH. Previous studies have demonstrated that FeNPs exhibit excellent antioxidant activities. They effectively scavenge free radicals by either transferring hydrogen atoms or donating electrons to free radicals (Bouafia *et al*. 2021). Consequently, FeNPs can disrupt the oxidation process, thereby preventing oxidative damage to proteins, nucleic acids, carbohydrates, and lipids (Kumar *et al*. 2020).

Table 2 presents the results of the FRAP assay for AgNPs and FeNPs. FeNPs demonstrated a higher capacity to reduce Fe^{3+} to Fe^{2+} ions, with values ranging from 32.17% to 61.20%, while AgNPs exhibited values from 33.60% to 78.39%. In the phosphomolybdenum assay, AgNPs showed a higher ability to reduce Mo (VI) to Mo (V) ions, achieving a range of 86.41% to 94.01%, compared to FeNPs, which ranged from 10.18% to 72.53%.

Foodborne pathogens such as *Campylobacter* spp., *E. coli, S. aureus, Salmonella* spp., and *Yersinia enterocolitica* pose a significant threat to public health (Bintsis 2017). Research studies have identified silver (Ag) and gold (Au) NPs as promising antimicrobial agents due to their effectiveness against a wide range of pathogenic microbes (Rabiee *et al.* 2022, Balestri *et al.* 2023). Numerous research studies have investigated the antioxidant and antimicrobial activities of nanoparticles synthesized from various fruit peels. Jackfruit was chosen for this study due to the substan-

Table 3. Antimicrobial activity of NPs synthesized from JFPE.

Bacterial strains	Tetracycline	AgNPs 250 µg	500 µg	1000 µg	FeNPs 250 µg	500 µg	1000 µg
			Antibacterial activity				
Escherichia coli	23	18	18	20	-	13	14
Bacillus subtilis	22	17	19	20	14	15	17
Enterococcus faecalis	20	17	18	19	13	14	20
Staphylococcus aureus	23	21	22	23	-	-	11
Streptococcus mutans	25	22	23	24	-	-	6
Pseudomonas aeruginosa	23	21	22	23	-	-	13
			Antifungal activity				
Fungal strains	Fluconazole	250 µg	500 µg	1000 µg	250 µg	500 µg	1000 µg
Candida krusei	20	11	11	12	-	-	-
Candida tropicalis	19	15	15	16	-	-	-
Candida albicans	21	13	13	14	-	-	-

tial waste it produces, primarily in the form of peels, and rind, rendering it an abundant and underutilized resource for green nanoparticle synthesis.

The antimicrobial activity of NPs synthesized from JFPE is presented in Table 3. Comparing the antibacterial effects of the synthesized NPs, AgNPs demonstrated a stronger concentration-dependent antibacterial effect against both gram-positive and gram-negative bacterial strains. The highest activity was recorded against *Streptococcus mutans*, followed by *Pseudomonas aeruginosa* and *Staphylococcus aureus.* In contrast, antifungal activity was observed solely for AgNPs. AgNPs exhibit antibacterial activity by disrupting the structure and permeability of bacterial cell membranes. They interact with sulfur or phosphorus groups in intracellular molecules such as DNA and proteins. They can alter the respiratory chain by targeting thiol groups in enzymes. Furthermore, AgNPs can interfere with cellular components, which subsequently alters the metabolic pathways, and genetic material, ultimately leading to cell death (Gomaa 2017, Bruna *et al*. 2021).

CONCLUSION

The findings highlight the potential of fruit waste extracts as valuable resources for the synthesis of green nanoparticles. Silver and iron nanoparticles were successfully synthesized using jackfruit peel extract, which showed remarkable antioxidant and antimicrobial properties. These nanoparticles present significant opportunities for applications in the food industry, particularly in the development of biodegradable food films and sustainable packaging materials, thereby promoting an environmentally friendly and sustainable economy.

ACKNOWLEDGMENT

The authors sincerely thank Armats Biotek Laboratories for providing the essential research facilities.

ABBREVIATIONS

PMS: Phenazine methosulfate
NADH: Nicotinamide adenine dinucleotide
NBT: Nitro blue tetrazolium
PBS: Phosphate buffer solution
$K_3[Fe(CN)_6]$: Potassium ferricyanide
TCA: Trichloro acetic acid
$FeCl_3$: Ferric chloride
Na_3PO_4: Sodium phosphate
$(NH_4)_2MoO_4$: Ammonium molybdate

REFERENCES

Adan, A. A., Ojwang, R. A,, Muge, E. K., Mwanza, B. K., & Nyabaga, E. N. (2020). Phytochemical composition and essential mineral profile, antioxidant and antimicrobial potential of underutilized parts of jack fruit. *Food Research*, 4(4), 1125-134. https://doi.org/10.26656/fr.2017.4(4).326

Balestri, A., Cardellini, J., & Berti, D. (2023). Gold, and silver nanoparticles as tools to combat multi-drug-resistant pathogens. *Current Opinion in Colloid and Interface Science,* 66: 101710. https://doi.org/10.1016/j.cocis.2023.101710

Banu, S. A., John, S., Sarah, J. M., Saraswathi, K., & Arumugam, P. (2021). Screening of secondary metabolites, bioactive compounds, *in vitro* antioxidant, antibacterial, antidiabetic and anti-inflammatory activities of chia seeds (*Salvia hispanica* L.). *Research Journal of Pharmacy and Technology*, 14(12), 6289-6294. https://doi.org/10.52711/0974-360X.2021.01088

Begam, A. S., John, S., Monica, S. J., Priyadarshini, S., Sivaraj, C., & Arumugam, P. (2020). *In vitro* antioxidant activity and GC-MS analysis of peel and pulp extracts of *Dimocarpus longan. International Journal of Biology, Pharmacy, and Allied Sciences*, 9(6), 1269-1283. https://doi.org/10.31032/IJBPAS/2020/9.6.5071

Bintsis, T. (2017). Foodborne pathogens. *AIMS Microbiology*, 29: 3(3), 529-563. https://doi.org/10.3934/microbiol.2017.3.529

Bouafia, A., Laouini, S. E., Khelef, A., Tedjani, M. L., & Guemari, F. (2021). Effect of ferric chloride concentration on the type of magnetite (Fe_3O_4) nanoparticles biosynthesized by aqueous leaves extracts of Artemisia and assessment of their antioxi dant activities. *Journal of Cluster Science,* 32, 1033-1041

Brahma, R., & Ray, S. (2022). In-depth analysis on potential applications of jackfruit peel waste. A systematic approach. *Food Chemistry Advances* 1, 100119. https://doi.org/10.1016/j.focha 2022.100119

Bruna, T., Maldonado-Bravo, F., Jara, P., & Caro, N. (2021). Silver nanoparticles and their antibacterial applications. *International Journal of Molecular Sciences,* 22(13), 7202. https://doi.org/10.3390/ijms22137202

Faghihi, R., Larijani, K., Abdossi, V., & Moradi, P. (2020). Silver nanoparticles produced by green synthesis using Citrus para dise peel inhibits *Botryytis cinerea in vitro*. *Journal of Hor ticulture and Postharvest Research,* 3,151-160. https://doi.org/10.22077/jhpr.2019.2540.1063

Fahmy, H. M., Mohamed, F. M., Marzouq M. H., Mustafa A. B. E., Alsoudi, A. M., Ali, O. A., Mohamed, M. A., & Mahmoud, F. A. (2018). Review of green methods of iron nanoparticles synthesis and applications. *Bio Nanoscience*, pp 491–503.

https://doi.org/10.1007/s12668-018-0516-5

Gabriel, T., Vestine, A., Kim, K. D., Kwon, S. J., Sivanesan, I., & Chun, S. C. (2022). Antibacterial activity of nanoparticles of garlic (*Allium sativum*) extract against different bacteria such as *Streptococcus mutans* and *Poryphormonas gingivalis*. *Applied Sciences,* 12(7), 3491. https://doi.org/10.3390/app12073491

Gizaw, A., Marami, L. M., Teshome, I., Sarba, E. J., Admasu, P., Babele, D. A., Dilba, G. M,, Bune, W. M., Bayu, M. D., Tadesse, M., & Abdisa, K. (2022). Phytochemical screening and *in vitro* antifungal activity of selected medicinal plants against *Candida albicans* and *Aspergillus niger* in West Shewa Zone, Ethiopia. Advances in Pharmacological and Pharma ceutical Science, pp 3299146. https://doi.org/10.1155/2022/3299146

Gomaa, E. Z. (2017). Silver nanoparticles as an antimicrobial agent: A case study on *Staphylococcus aureus* and *Escherich ia coli* as models for Gram-positive and Gram-negative bacteria. *The Journal of General and Applied Microbiology* 63(1), 36-43. https://doi.org/10.2323/jgam.2016.07.004

Khan, I., Saeed, K., & Khan, I. (2019). Nanoparticles: Properties, applications, and toxicities. *Arabian Journal of Chemistry,* 12 (7), 908-931. https://doi.org/10.1016/j.arabjc.2017.05.011

Kumar, H., Bhardwaj, K., Nepovimova E., Kuca, K., Dhanjal, D. S., Bhardwaj, S., Bhatia, S. K., Verma, R., & Kumar, D. (2020). Antioxidant functionalized nanoparticles: A combat against oxidative stress. *Nanomaterials*, 10, 1-31

Kumar, H., Bhardwaj, K., Sharma, R., Nepovimova, E., Kuca, K., Dhanjal, D. S., Verma, R., Bhardwaj, P., Sharma, S., Kumar, D. (2020). Fruit and vegetable peels: Utili zationn of high-value horticultural waste in novel industrial applications. *Molecules*, 25(12), 2812. https://doi.org/10.3390/molecules25122812

Leta, T. B., Adeyemi, J. O., & Fawole, O. A. (2024). Utilizing fruit waste-mediated nanoparticles for sustainable food pack aging materials to combat food loss and waste. *Food Bioscience,* 59, 104151. https://doi.org/10.1016/j.fbio.2024.104151

Magdy, G., Aboelkassim, E., Elhaleem, S. M. A., & Belal, F. (2024). A comprehensive review on silver nanoparticles: Synthesis approaches, characterization techniques, and recent pharmaceutical, environmental, and antimicrobial aplications. *Microchemical Journal*, 196, 109615. https://doi.org/10.1016/j.microc.2023.109615

Mzoughi, Z., Chahdoura, H., Chakroun, Y., Camara, M., Fernandez-Ruiz, V., Morales, P., Mosbah, H., Flamini, G., Snoussi, M., & Majdoub, H. (2019). Wild edible Swiss chard leaves (*Beta vulgaris* L. var. cicla): Nutritional, phytochemical composition and biological activities. *Food Research International,* 119, 612–621. https://doi.org/10.1016/j.foodres.2018.10.039

Nirmal, N. P., Khanashyam, A. C., Mundanat, A. S., Shah, K., Babu, K. S., Thorakkattu, P., Al-Asmari, F., & Pandisevam, R. (2023). Valorization of Fruit Waste for Bioactive Compounds and Their Applications in the Food Industry. Foods, 12(3), 556. https://doi.org/10.3390/foods12030556

Prieto, P., Pineda, M., & Aguilar, M. (1999). Spectrophotometric quantitation of antioxidant capacity through the formation of a phosphomolybdenum complex: specific application to the determination of vitamin E. *Analytical Biochemistry*, 269(2): 337-341. https://doi.org/10.1006/abio.1999.4019

Rabiee, N., Ahmadi, S., Akhavan, O., & Luque, R. (2022). Silver and gold nanoparticles for antimicrobial purposes against multi-drug resistance bacteria. *Materials* 15(5), 1799. https://doi.org/10.3390/ma17122841

Ranasinghe, R. A. S. N., Maduwanthi, S. D. T., & Marapaana, R. A. U. J. (2019) Nutritional and health benefits of jackfruit (*Artocarpus heterophyllus* Lam): A review. *Intenational Journal of Food Science*, 4327183. https://doi.org/10.1155/2019/4327183

Rodriguez-Felix, F., Graciano-Verdugo, A. Z., Moreno-Vasquez, M. J., Lagarda-Diaz, I., Barreras-Urbina, C. G., Armenta-Vil legas, L., Olguin-Moreno, A., Tapia-Hernandez, J. A. (2023). Trends in sustainable green synthesis of silver nanoparticles using agri-food waste extracts and their applications in health. *Journal of Nanomaterial*. https://doi.org/10.1155/2022/8874003

Sangeetha, S. T., John, S., Monica, S. J., Arumugam, P. (2020). Phytochemical profile and biological properties of pulp and peel extracts of *Docynia indica* (Wall) Decne – An endemic wild fruit of North East India. *World Journal of Environmental Biosciences,* 9(2), 62-70.

Suhag, R., Kumar, R., Dhiman, A., Sharma, A., Prabhakar, P. K., Gopalakrishnan, K., Kumar, R., Singh, A. (2022). Fruit peel bio-actives, valorization into nanoparticles and poten tial applications. A review. *Critical Reviews in Food Science and Nutrition*, 63(24), 6757-6776. https://doi.org/10.1080/10408398.2022.2043237

Xu, S.Y., Liu, J. P., Huang, X., Du, L. P., Shi, F. L., Dong, R., Huang, X. T., Zheng, K., Liu, Y., & Cheong, K. L. (2018). Ultrasonic microwave-assisted extraction, characterization, and biological activity of pectin from jackfruit peel. LWT *Food Science and Technology*, 90, 577-582. https://doi.org/10.1016/j.lwt.2018.01.007